Energy Scheduling for a Smart Home Applying Stochastic Model Predictive Control

Mehdi Rahmani-andebili and Haiying Shen
Department of Electrical and Computer Engineering
Clemson University, Clemson, SC 29631, USA
mehdir@g.clemson.edu, shenh@clemson.edu

***Abstract*- A smart home (SH) can have a variety of sources such as diesel generator (DG), photovoltaic (PV) panels installed on the roof of the SH, and plug-in electric vehicle (PEV) as an energy storage. In addition, a SH is able to transact power with the local distribution company (DISCO) through the grid. This study intends to investigate the energy scheduling problem of a SH so that the daily electricity consumption cost of the SH is minimized. Herein, the challenges include modeling the economic and technical constraints of the DG and the battery of the PEV, and also dealing with the variability and uncertainties concerned with the power of the PV panels that make the problem a nonlinear, dynamic (time-varying), and stochastic optimization problem. In order to handle the variability and uncertainties of the power of the PV panels, a stochastic model predictive control (MPC) is applied. Herein, a combination of genetic algorithm (GA) and linear programming (GA-LP) approach is applied as the optimization tool. The numerical study demonstrates the competence of the proposed approach for decreasing the operation cost.**

***Index Terms*- Energy scheduling, photovoltaic (PV) panels, plug-in electric vehicle (PEV), smart home (SH), and stochastic model predictive control (MPC).**

I. Introduction

In order to calm the energy security and environmental issues caused by burning fossil fuels in the thermal power plants, installing renewable energy resources, especially photovoltaic (PV) panels, in the residential building is proposed, since solar energy is the most cost-effective and carbon-free source of energy [1]. Advances in the technology promise that every home can be changed into a smart home (SH) that allows the occupant to control the energy consumption of the home remotely [2-4]. In addition, a SH can deliver its extra energy to the grid and sell it to the local distribution company (DISCO), but at a lower price compared to the purchasing price from the local DISCO [5].

SHs have a huge potential for decreasing cost of energy use, increasing energy efficiency, decreasing the carbon footprint by including renewables, and transforming the role of the occupant [6]. The importance of energy scheduling of the SHs can be inferred from the statistical information which indicates that the electricity consumption in the residential sector represents over 30% of the energy consumption of the world [7]. The U.S. Energy Information Administration (EIA) estimates that 37% of end use electricity in the U.S. is consumed in the residences [8]. Also, the buildings are responsible for 36% of the carbon emissions in the U.S. [8-9].

Herein, an important question for energy scheduling problem of a SH is: *At every time step, how much energy to use from the available energy sources of the SH such as diesel generator (DG), renewables (PV panels), and energy storage (battery), and how much energy to purchase/sell from/to the local DISCO to supply the demanded energy of the SH so that the daily energy consumption cost of the SH is minimized.* In this paper, a SH predicts the power of the PV panels installed on the roof of the SH, takes into account its available energy resources, and conducts the energy scheduling. However, there exist several challenges in solving the problem listed below.

- Renewable energy resources such as PV panels have the features of uncertainty and variability in their power that makes the energy scheduling problem a stochastic and dynamic (time-varying) optimization problem.
- There are several economic and technical constraints for the DG and the battery of plug-in electric vehicle (PEV) such as the power limits and minimum up/down time limits of the DG, power limits of the battery of the PEV, state of charge (SOC) limit and depth of discharge (DOD) limit of the battery of the PEV, life loss cost of the battery of the PEV, and unavailability of the PEV for the SH when the PEV is being used by the driver. These aspects make the problem a mixed integer nonlinear programming (MINLP) problem.

There are some papers that have investigated energy scheduling problem a SH [10-13]. However, these studies have not considered some of the aforementioned aspects of the problem. In [10] and [12-13], the presence of different energy resources have not been modeled in the problem. In other words, renewable energy resources have been disregarded in [10] and [12-13], energy storage has not been modeled in [10] and [13], and presence of DG has not been taken into consideration in [10]. Also, the defined energy scheduling problem does not have any dynamic and adaptive characteristics in the studies [11-12]. In other words, the problem has been optimized once for the whole operation period (one day), while the optimization of the problem must be updated at every time step (e.g., every hour, every five minutes, or …) due to the time-varying feature of the power of renewables or load demand.

The paper is organized as follows. In Section II, the proposed technique for solving the energy scheduling problem of a SH is presented. In Section III, the problem is formulated. The numerical study is done in Section IV, and finally Section V concludes the paper.

II. Proposed Technique

In this section, different parts of the proposed technique for solving the energy scheduling problem of the SH is presented and described. Fig. 1 illustrates the configuration and different parts of the proposed approach.

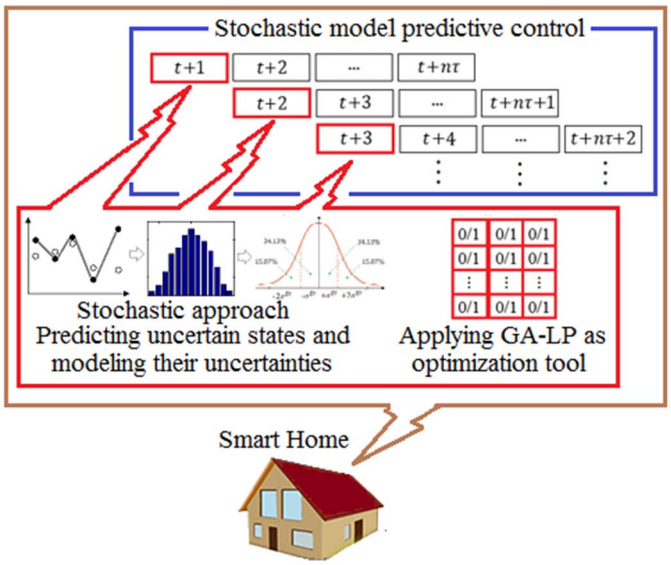

Fig. 1. Different parts of the proposed approach for solving the energy scheduling problem of the SH.

A. Stochastic Model Predictive Control

In this study, in order to address the variability and uncertainties concerned with the power of the PV panels a stochastic model predictive control (MPC) is applied.

1) Forecasting value of the uncertain states

The uncertain states of the problem that include values of the solar irradiances (ρ) over the optimization time horizon $(t+1,\cdots,t+n_\tau)$ are predicted using the neural network available in MATLAB. The value of n_τ is 12, since the duration of the optimization time horizon is assumed to be twelve time steps. Also, it should be noticed that the operation time period of the problem $(1,\cdots,n_t)$ is one day, thus n_t is equal to 288 because the duration of every time step (t) is 5 minutes.

The historical values of solar irradiances are used as the entries for the neural network to predict the values of solar irradiances over the optimization time horizon. The historical data related to the values of the solar irradiances are the real solar irradiances recorded in Clemson, SC 29634, USA in July 2014. Also, about 70% of the data is used for training the neural network and 30% of the data is used for validation and testing. The set of the predicted solar irradiances ($\tilde{\rho}$) in the SH can be presented as (1).

$$\{\tilde{\rho}_{t+1},\dots,\tilde{\rho}_{t+n_\tau}\},\forall t\in T, T=\{1,\cdots,n_t\} \qquad (1)$$

2) Modeling uncertainties of the forecasted data

Fig. 2 (a) illustrates the predicted and measured solar irradiances for the current time step (t) and past time steps $(1,2,\cdots,t-1)$, and also the predicted solar irradiances for every time step of the optimization time horizon $(t+1,\cdots,t+n_\tau)$. As can be seen, the previously forecasted solar irradiances ($\tilde{\rho}$) are compared with the real solar irradiances (measured data) and the value of error of the predictions are calculated. Then, as can be seen in Fig. 2 (b), redundancy of the prediction errors respect to the value of the prediction errors are plotted on a chart. After that, an appropriate probability density function is found for the prediction errors, as can be seen in Fig. 2 (c). It is observed that the predication errors can be precisely fitted on a Gaussian probability density function with an appropriate standard deviation (σ^{Er}) and a mean value equal to almost zero [14]. Finally, the curve is divided into four areas to define four distinct values for the prediction inaccuracy with occurrence probabilities about 15.87%, 34.13%, 34.13%, and 15.87% related to $-2\sigma^{Er}$, $-\sigma^{Er}$, σ^{Er}, and $2\sigma^{Er}$, respectively. The value of σ^{Er} is updated in the next predictions in the optimization procedure of the problem $(1,2,\cdots,t,\cdots,288)$.

Although considering more scenarios for the value of solar irradiance over the optimization time horizon will result in more accurate outcomes for the problem, it may lead to an unmanageable optimization problem. In other words, the optimization problem cannot be solved due to the large number of the scenarios in the desirable time. This phenomenon happens because of the short time step (five minutes) considered in the optimization procedure of the problem, and also because of the application of MPC (the optimization problem must be updated at every time step). Therefore, in order to avoid dealing with an unmanageable optimization problem, four scenarios for solar irradiance corresponding to $\rho_t\in\{\tilde{\rho}_t-2\sigma^{Er},\tilde{\rho}_t-\sigma^{Er},\tilde{\rho}_t+\sigma^{Er},\tilde{\rho}_t+2\sigma^{Er}\}$ with occurrence probabilities (Ω^{PV}) 15.87%, 34.13%, 34.13%, and 15.87%, respectively, are considered. In other words, at every time step, the problem is solved four times and every time, one of the above mentioned values are considered for the value of the solar irradiance.

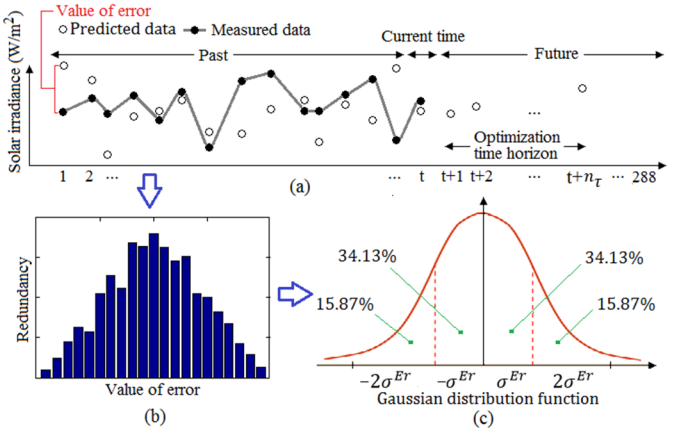

Fig. 2. (a): The predicted data, measured data, and value of prediction error (b): The redundancy of the prediction errors respect to the value of the prediction errors. (c): The Gaussian probability density function proportional to the prediction errors.

3) Model predictive control

MPC as a well-established method in control engineering is capable of controlling a multi-variable constrained system by taking the control actions from the solution of an online optimization problem and repetitively predicting the system behavior [15]. The concept of the applied MPC is illustrated in Fig. 3 [16]. As can be seen, at every time step (t), the optimization time horizon $(t+1,\cdots,t+n_\tau)$ is updated, and then the value of the forward-looking objective function (F_t^{FL}) is minimized; however, just the variables of the next time step $(t+1)$ are accepted as the decision variables. The forward-looking objective function is sum of the values of the time step objective functions (F_t) over the optimization time horizon, as can be seen in (1). Next, the current time step is $t+1$ and the updated optimization time horizon is $t+2,\cdots,t+n_\tau+1$. Now, the value of the updated forward-looking objective

function (F_{t+1}^{FL}) is minimized and the variables of the next time step $(t+2)$ are accepted as the decision variables. This procedure that demonstrates the dynamic and adaptability characteristics of the MPC is repeated for every time step of the operation period $(1, \cdots, n_t)$.

$$F_t^{FL} = \sum_{\tau=1}^{n_\tau} F_{t+\tau}, \forall t \in T \quad (1)$$

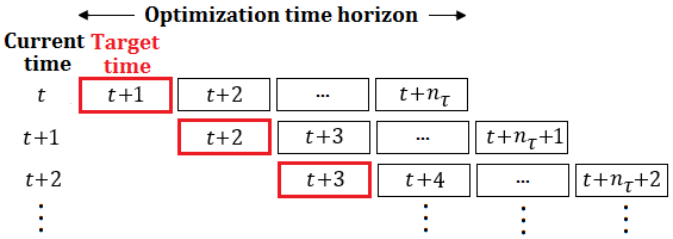

Fig. 3. The concept of the model predictive control [16].

B. Optimization Tool

The energy scheduling problem of the SH is a MINLP problem. In this study, GA-LP technique as the combination of genetic algorithm (GA) and linear programming (LP) is applied to solve the energy scheduling problem of the SH. Other optimization algorithms could be used instead of GA; however, the capability of GA for parallel optimization and its competence in complex and nonlinear environments are the main reasons for the utilization of GA [17].

Herein, the GA is applied to address the nonlinearity of the problem and the LP is applied to quickly find the globally optimal solution. Moreover, the GA and LP techniques deal with the discrete variables and the continuous variables of the problem, respectively.

The discrete variables of the problem handled by the GA include the status of the DG (x^{DG}) and the status of the battery of the PEV (x^{PEV}) in every time step of the optimization time horizon, as can be seen in (2). Herein, values of "0" and "1" for x^{DG} mean "off" and "on", respectively. Also, values of "-1", "0", and "1" for x^{PEV} mean charging, idle, and discharging, respectively.

$$\begin{Bmatrix} x_t^{DG} & \cdots & x_{t+n_\tau}^{DG} \\ x_t^{PEV} & \cdots & x_{t+n_\tau}^{PEV} \end{Bmatrix}, \forall t \in T \quad (2)$$

Based on this, the dimensions of the defined chromosome in the applied GA are $n_\tau \times 3$, as can be seen in Fig. 4. Herein, one bit (gene) for indicating status of the DG ("0" for "off" and "1" for "on") and two bits for indicating the status of the battery of the PEV ("00" and "10" for idle, "01" for discharging, and "11" for charging) are considered.

In addition, the continuous variables of the problem optimized by the LP include the value of power of the DG (P^{DG}), the value of generated or consumed power of the battery of the PEV (P^{PEV}), and the value of transacted power with the DISCO through the electricity grid (P^{Grid}) in every time step of the optimization time horizon, as can be seen in (3).

$$\begin{Bmatrix} P_t^{DG} & \cdots & P_{t+n_\tau}^{DG} \\ P_t^{PEV} & \cdots & P_{t+n_\tau}^{PEV} \\ P_t^{Grid} & \cdots & P_{t+n_\tau}^{Grid} \end{Bmatrix}, \forall t \in T \quad (3)$$

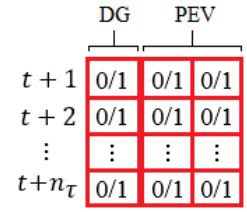

Fig. 4. The structure of the defined chromosome in the applied GA.

III. Problem Formulation

A. Objective Function

The goal of the SH is minimizing the value of the stochastic forward-looking objective function over the optimization time horizon ($\mathbb{F}^{FL}$) subject to the constraints presented in (11)-(19). As can be seen in (4), the value of the stochastic forward-looking objective function is determined by summing the values of the forward-looking objective functions (F^{FL}) weighted by the corresponding occurrence probability (Ω^{PV}). In other words, the value of the stochastic forward-looking objective function ($\mathbb{F}^{FL}$) is the expected value of the forward-looking objective function (F^{FL}). The forward-looking objective function ($F_t^{FL} = \sum_{\tau=1}^{n_\tau} F_{t+\tau}$) has been presented in (1). The time step objective function (F) that includes different cost and income terms is presented in (5). These terms include fuel cost of the DG (C^{F_DG}), carbon emissions cost of the DG (C^{E_DG}), start up cost of the DG (C^{STU_DG}), shut down cost of the DG (C^{SHD_DG}), switching cost of the battery of the PEV (C^{SW_PEV}), and cost or benefit due to power transactions with the local DISCO through the grid ($P^{Grid} \times \acute{\pi}^{DISCO}$).

$$min\, \mathbb{F}_t^{FL} = min \sum_{P_t^{PV}} F_t^{FL} \times \Omega_t^{PV}, \forall t \in T \quad (4)$$

$$F_t = \begin{Bmatrix} [C_t^{F\_DG}] + [C_t^{E\_DG}] \\ +[(1 - x_{t-1}^{DG}) \times x_t^{DG} \times C^{STU\_DG}] \\ +[x_{t-1}^{DG} \times (1 - x_t^{DG}) \times C^{SHD\_DG}] \\ +[\acute{x}_t^{PEV} \times C^{SW\_PEV}] + [P_t^{Grid} \times \acute{\pi}_t^{DISCO}] \end{Bmatrix}, \forall t \in T \quad (5)$$

where,

$$\acute{x}_t^{PEV} = \begin{cases} 0 & x_{t-1}^{PEV} = x_t^{PEV} \\ 1 & x_{t-1}^{PEV} \neq x_t^{PEV} \end{cases}, \forall t \in T \quad (6)$$

$$\acute{\pi}_t^{DISCO} = \begin{cases} \pi_t^{DISCO} & P_t^{Grid} > 0 \\ \varphi \times \pi_t^{DISCO} & P_t^{Grid} < 0 \end{cases}, \forall t \in T \quad (7)$$

The switching of the battery of the PEV is determined using (6). If the status of the battery in the current time step (x_t^{PEV}) is the same as the previous time step (x_{t-1}^{PEV}), the switching indicator ($\acute{x}^{PEV}$) is zero; otherwise, it is one.

In (7), φ is the coefficient applied by the local DISCO to determine the price of selling power to the local DISCO by the SH based on the net energy metering (NEM) plan [5]. In the NEM plan, the SH can deliver its extra power to the grid and sell it to the local DISCO at a lower price compared to the purchasing price from the local DISCO [5]. Herein, $P^{Grid} > 0$ means the SH purchases power from the local DISCO and $P^{Grid} < 0$ means the SH sells power to the local DISCO.

The fuel cost function and carbon emissions function of a DG are quadratic polynomials presented in (8) and (9), respectively [18-19]. Herein, the set of z_1^F, z_2^F, z_3^F and z_1^E, z_2^E, z_3^E are the fuel cost coefficients and carbon emissions coefficients of the DG, respectively. Also, β^E is the value of penalty for carbon emissions.

$$C_t^{F\_DG} = x_t^{DG} \times (z_1^F \times (P_t^G)^2 + z_2^F \times (P_t^G) + z_3^F), \forall t \in T \quad (8)$$

$$C_t^{E\_DG} = x_t^{DG} \times \beta^E \times (z_1^E \times (P_t^G)^2 + z_2^E \times (P_t^G) + z_3^E), \quad \forall t \in T \quad (9)$$

The value of the switching cost of the battery of a PEV is determined based on the value of total cumulative ampere-hours throughput of the battery (ξ^{PEV}) in its life cycle and the value of the initial price of the battery (Pr^{PEV}). In fact, considering this cost term prevents the battery of the PEV from unnecessary switching that is harmful to its life span.

$$C^{SW\_PEV} = \frac{Pr^{PEV}}{\xi^{PEV}} \quad (10)$$

B. Constraints

In the following, the constraints of the problem that must be held at every time step of the operation period are presented and described.

1) Supply-demand balance

The sum of power of the DG, the power of the PV panels, the power of the battery of the PEV, and the transacted power with the local DISCO through the grid must be equal to the load demand of the SH (D^L) at every time step of the operation period.

$$(x_t^{DG} \times P_t^{DG}) + (x_t^{PEV} \times P_t^{PEV}) + P_t^{PV} + P_t^{Grid} = D_t^L, \quad \forall t \in T \quad (11)$$

The output power of the PV panels is a nonlinear function of the estimated solar irradiance (ρ), as can be seen in (12) [20]. Herein, ρ^s and ρ^c are the solar irradiance in the standard environment set as 1000 W/m^2 and certain solar irradiance point set as 150 W/m^2, respectively. Also, $\overline{P^{PV}}$ indicates the rated power of the PV panels.

$$P_t^{PV} = \begin{cases} \overline{P^{PV}} \times \dfrac{(\rho_t)^2}{\rho^s \times \rho^c} & \rho_t \le \rho^c \\ \overline{P^{PV}} \times \dfrac{\rho_t}{\rho^s} & \rho_t > \rho^c \end{cases}, \forall t \in T \quad (12)$$

2) Power limits of the diesel generator

The maximum power limit ($\overline{P^{DG}}$) and minimum power limit ($\underline{P^{DG}}$) of the DG is presented in (13). In other words, the DG cannot generate power beyond limits.

$$x_t^{DG} \times \left(\underline{P^{DG}} \le P_t^{DG} \le \overline{P^{DG}}\right), \forall t \in T \quad (13)$$

3) Minimum up/down time limits of the diesel generator

The duration that the DG is continuously "on" (Δt^{DG_ON}) and "off" (Δt^{DG_OFF}) must be more than the rated minimum up time (MUT^{DG}) and minimum down time (MDT^{DG}), respectively. In other words, the DG cannot be started up immediately after it has been shut down and vice versa. Also, the time interval that the DG is continuously "on" (or "off") is determined based on the time that has passed from the last start up time (or shut down time) of the DG.

$$\Delta t^{DG\_ON} \ge MUT^{DG} \quad (14)$$

$$\Delta t^{DG\_OFF} \ge MDT^{DG} \quad (15)$$

4) Power limits of the battery of the PEV

The battery of the PEV can act as a load or a generator by being charged or discharged, respectively; however, the value of power of the battery of the PEV must be in the rated range. Herein, $\overline{P^{PEV}}$ is the value of rated power of the battery of the PEV.

$$x_t^{PEV} \times \left(-\overline{P^{PEV}} \le P_t^{PEV} \le \overline{P^{PEV}}\right), \forall t \in T \quad (16)$$

5) Depth of discharge limit of the battery of the PEV

In order to prolong the life time of the battery of the PEV, the battery must not be discharged more than the allowable DOD. Moreover, the battery has a definite capacity that cannot be charged more than that.

$$DOD^{PEV} \le SOC_t^{PEV} \le 100, \forall t \in T \quad (17)$$

6) Disconnection of the PEV from the SH

This constraint indicates that the PEV is being used by its driver and the PEV is no longer connected to the SH in this interval ($\Delta t_{Dep-Arr}$), as can be seen in (18). In other words, the SH does not have any energy storage, thus the status of the battery of the PEV is zero at these time steps.

$$x_t^{PEV} = 0, t \in \{\Delta t_{Dep-Arr}\} \quad (18)$$

7) Full charge constraint for the battery of the PEV before departure

By holding this constraint, the owner of the PEV is confident that the PEV will have full charge at the desirable time (t_{Dep}) and ready to be used. In other words, the occupant of the SH prefers to have full charge in the battery of the PEV before driving the PEV.

$$SOC_{t_{Dep}}^{PEV} = 100 \quad (19)$$

IV. Numerical Study

The problem simulation is done in MATLAB environment using the Intel Xeon Sever with 64 GB RAM.

A. Characteristics of the case study

Fig. 5 illustrates the configuration of the case study that includes a SH with different sources including PV panels installed on the roof of the SH, PEV, DG, and electrical distribution grid. The technical data of the DG is presented in TABLE I. Furthermore, the value of other parameters of the problem are presented in TABLE II. The value of penalty for carbon emissions (β^E) is based on the introduced value by California Air Resources Board auction of greenhouse gas emissions [21]. In TABLE II, Cap^{PEV} indicates the value of capacity of the battery of the PEV. Also, t_{Arr} and t_{Dep} are the time that the PEV is connected/disconnected to/from the SH by the occupant, respectively. In addition, n_c and θ^{Mut} are the number of chromosomes in the population and the value of mutation probability of the genes in the applied GA.

Fig. 6 shows the electricity price proposed by the local DISCO in every time step (five minutes) of the operation

period (one day). Moreover, the load demand of the SH at every time step of the operation period is presented in Fig. 7. In addition, power pattern of the PV panels of the SH is shown in Fig. 8. The standard deviation of the prediction errors related to the solar irradiance is considered about 5%.

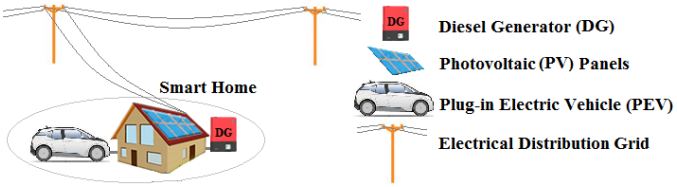

Fig. 5. The configuration of the case study.

TABLE I
THE TECHNICAL DATA OF THE DIESEL GENERATOR.

Parameter	Value	Parameter	Value
z_1^F (¢/kWh^2)	0.00491	P^{DG} (kW)	5
z_2^F (¢/kWh)	7.85	$\overline{P^{DG}}$ (kW)	20
z_3^F (¢)	0	MUT^{DG} (min)	10
z_1^E (kg/kWh^2)	0.0008	MDT^{DG} (min)	10
z_2^E (kg/kWh)	0.61	C^{STU_DG} (¢)	100
z_3^E (kg)	0	C^{SHD_DG} (¢)	100

TABLE II
THE VALUE OF PARAMETERS OF THE PROBLEM.

n_t	288	$\overline{P^{PEV}}$ (kWh)	10	Pr^{PEV} (¢)	200,000
t	5 min	Cap^{PEV} (kWh)	50	ξ^{PEV} (Ah)	10,000
n_τ	12	DOD^{PEV} (%)	20	θ^{Mut} (%)	5
φ	0.8	$SOC_{t_{Dep}}^{PEV}$ (%)	100	n_c	50
β^E (¢/kg)	1	$SOC_{t_{Arr}}^{PEV}$ (%)	80		
$\overline{P^{PV}}$ (kW)	10	$\Delta t_{Dep-Arr}$	9-10, 16-17		

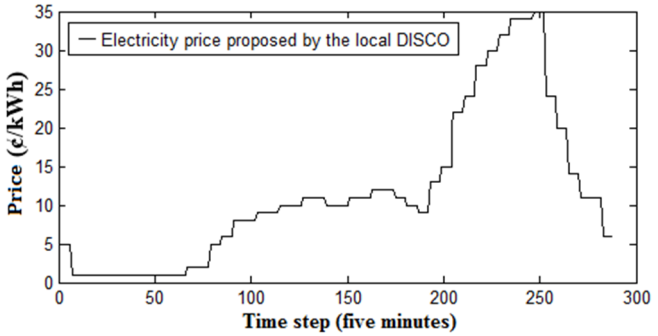

Fig. 6. The electricity price proposed by the local DISCO at every time step of the operation period.

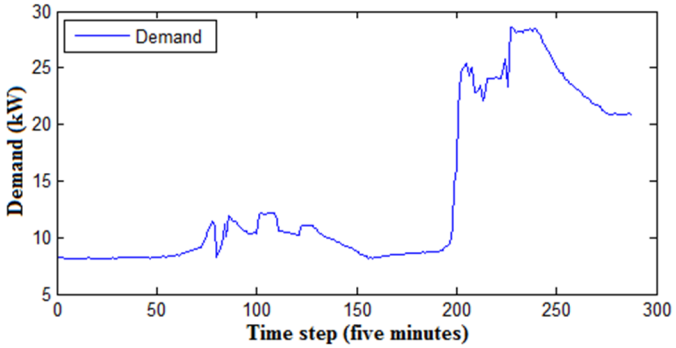

Fig. 7. The load demand of the SH at every time step of the operation period.

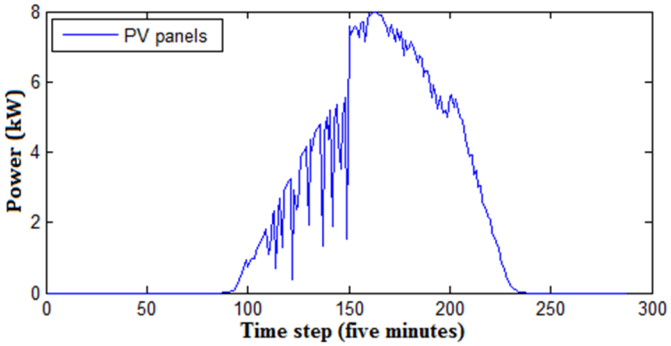

Fig. 8. The power pattern for the PV panels in a cloudy day at every time step of the operation period.

B. Problem simulation

Fig. 9 shows the optimally scheduled power for the sources of the SH (the battery of the PEV, DG, and the grid) at every time step (five minutes) of the operation period (one day). As can be seen, the battery of the PEV is charged and discharged between 121th-144th, 205th-228th, and 253th-264th time steps. Also, the DG is kept "off" until 108th time step, and then it is started up and is kept "on"; however, it is set at the minimum level in some periods of the operation period. In addition, the electricity is transacted between the SH and the local DISCO in some periods of the operation period.

The operation cost of the SH and the performance of the battery of the PEV and the DG without energy scheduling and with energy scheduling applying the stochastic MPC are presented in Table III. As can be seen, after optimally scheduling the energy resources of the SH, the operation cost of the SH is decreased from \$51.1/day to about \$29.8/day (41% reduction). In this condition, the battery of the PEV and the DG are applied about 12.5% and 52.6% of their capacities, respectively.

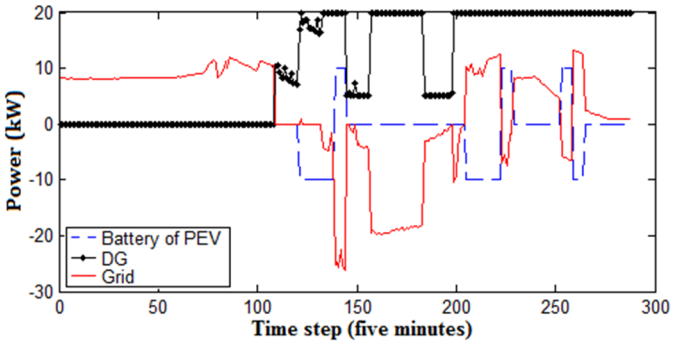

Fig. 9. The optimally scheduled power for the sources of the SH at every time step (five minutes) of the operation period (one day).

TABLE III
THE OPERATION COST OF THE SMART HOME (\$/DAY) BEFORE AND AFTER ENERGY SCHEDULING.

-	Before scheduling	After scheduling
Operation cost (\$/day)	51.1	29.8
Operation of the battery of the PEV (%)	0	12.5
Operation of the DG (%)	0	52.6

V. CONCLUSION

In this study, the stochastic model predictive control as the adaptive and dynamic optimization technique was applied in the energy scheduling problem of the smart home with

different sources of energy. Herein, the stochastic approach and model predictive control technique addressed the uncertainty and variability issues of the power of the PV panels, respectively.

It was proven that energy scheduling has a considerable potential for decreasing the daily operation cost of the SH. By the application of the MPC with five-minute time scale, the DG was able to adjust its output power within the small time step (five minutes). However, it was noticed that performance of the battery of the PEV as the energy storage was limited due to the short optimization time horizon (12 time steps, equal to one hour). Therefore, application of a multi-time scale MPC with short and long time scales are suggested as the extended work of the current study, since a multi-time scale MPC is capable of simultaneously having vast vision for the optimization time horizon and precise resolution for the problem variables.

ACKNOWLEDGMENTS

This research was supported in part by U.S. NSF grants NSF-1404981, IIS-1354123, CNS-1254006, IBM Faculty Award 5501145 and Microsoft Research Faculty Fellowship 8300751.

REFERENCES

[1] D. Pengwei, L. Ning. "Appliance commitment for household load scheduling," *IEEE Trans Smart Grid,* vol. 2, pp. 411-419, 2011.

[2] [Online]. Available: http://www.homes.com/blog/2012/08/7-recent-advances-in-home-security-technology/

[3] U.S. Congress, H. R. 6, "Energy Independence and Security Act of 2007," *110th Congress, 1st Session,* Jan. 4, 2007. [Online]. Available: http://www.gpo.gov/fdsys/pkg/BILLS-110hr6enr/pdf/BILLS-110hr6enr.pdf.

[4] L. Jiang, D. Y. Liu, and B. Yang, "Smart home research," *in Proc. 2004 Int. Conf. Mach. Learn. Cybern.,* vol. 2, pp. 659–663, 2004.

[5] Federal energy regulatory commission, [Online]. Available: http://www.ferc.gov/industries/electric/indus-act/section-1241.pdf.

[6] A. Zipperer, P. A. Aloise-Young, S. Suryanarayanan, R. Roche, L. Earle, D. Christensen, P. Bauleo, and D. Zimmerle, "Electric energy management in the SH: Perspectives on enabling technologies and consumer behavior," *Proceedings of the IEEE,* vol. 101, no. 11, pp. 2397-2408, 2013.

[7] N. Lior, "Sustainable energy development: the present (2009) situation and possible paths to the future," *Energy,* vol. 35, pp. 3976–3994, 2010.

[8] U.S. Energy Information Administration, "Annual energy review 2011," Washington, DC, EIA-0384, Sep. 2012.

[9] OECD/IEA, International Energy Agency, 2013. [Online]. Available: http://www.iea.org/aboutus/faqs/energyefficiency.

[10] Y. Liu, S. Hu, H. Huang, R. Ranjan, A. Y. Zomaya, and Lizhe Wang, "Game-theoretic market-driven SH scheduling considering energy balancing," *IEEE System Journal,* DOI: 10.1109/JSYST.2015.2418032.

[11] M. A. A. Pedrasa, T. D. Spooner, and I. F. MacGill, "Coordinated scheduling of residential distributed energy resources to optimize SH energy services, *IEEE Trans. Smart Grid,* vol. 1, no. 2, pp. 134-143, 2010.

[12] N. Gatsis and G. B. Giannakis, "Residential load control: Distributed scheduling and convergence with lost AMI messages," *IEEE Trans. Smart Grid,* vol. 2, no. 3, pp. 1–17, Feb. 2012.

[13] T. Chang, M. Alizadeh, and A. Scaglione, "Real-time power balancing via decentralized coordinated home energy scheduling," *IEEE Trans. Smart Grid,* vol. 4, pp. 1490-1504, 2013.

[14] M. Rahmani-andebili, "Spinning reserve supply with presence of plug-in electric vehicles aggregator considering compromise between cost and reliability, *IET Gener. Transm. Distrib.,* vol. 7, 2013, pp. 1442-1452.

[15] J. B. Rawlings and D. Q. Mayne, "Model predictive control: Theory and design," Nob Hill Publishing, LLC, Madison, WI, 2009. [Online]. Available: http://jbrwww.che.wisc.edu/home/jbraw/mpc/electronic-book.pdf.

[16] M. Rahmani-andebili, and G. K. Venayagamoorthy, Stochastic optimization for combined economic and emission dispatch with renewables, *IEEE Symposium Series on Computational Intelligence*, Cape Town, pp. 1252-1258, 2015.

[17] Mitchell, Melanie (1996). An Introduction to Genetic Algorithms. Cambridge, MA: MIT Press. ISBN 9780585030944.

[18] J. J. Grainger and W. D. Stevenson, Jr., Power System Analysis. New York: McGraw-Hill, 1994.

[19] A. J. Wood and B. F. Wollenberg, Power Generation, Operation and Control, 2nd ed. New York: Wiley, 1996.

[20] R. H. Liang and J. H. Liao, "A fuzzy-optimization approach for generation scheduling with wind and solar energy systems," *IEEE Trans. Power Syst.*, vol. 22, no. 4, pp. 1665-1674, Nov. 2007.

[21] U.S. energy information administration (EIA), [Online]. Available: http://www.eia.gov/todayinenergy/detail.cfm?id=9310. <Accessed Oct. 2015>.